Molecular Pharmacology Fast Forward. Published on March 19, 2009 as doi:10.1124/mol.109.054825

MOL #54825

Ligand Selectivity and Gene Regulation by the Human Aryl Hydrocarbon Receptor in Transgenic Mice

Colin A. Flaveny, Iain A. Murray, Chris R. Chiaro and Gary H. Perdew*

Center for Molecular Toxicology and Carcinogenesis and the Department of Veterinary and Biomedical Sciences, the Pennsylvania State University, University Park, Pennsylvania 16802

Molecular Pharmacology Fast Forward. Published on March 19, 2009 as DOI: 10.1124/mol.109.054825
This article has not been copyedited and formatted. The final version may differ from this version.

MOL #54825

Ligand Selectivity and Gene Regulation by the Human AHR

*Corresponding Author:

Gary H. Perdew

Center for Molecular Toxicology and Carcinogenesis

Department of Veterinary Science, Pennsylvania State University

309A Life Sciences Building, University Park, PA 16802

Phone: 814 865 0400
Fax: 814 863 1696
E-mail: ghp2@psu.edu

Number of text pages: 23

Number of tables: 1

Number of figures: 7

Number of references: 26

Number of words in abstract: 250

Number of words in introduction: 746

Number of words in discussion: 920

Abbreviations: PAL: 2-azido-3-[^{125}I]iodo-7,8-dibromodibenzo-*p*-dioxin, hAHR human aryl-hydrocarbon receptor, mAHR: mouse aryl hydrocarbon receptor

Molecular Pharmacology Fast Forward. Published on March 19, 2009 as DOI: 10.1124/mol.109.054825
This article has not been copyedited and formatted. The final version may differ from this version.

Abstract

The aryl hydrocarbon receptor (AHR) is a ligand inducible transcription factor that displays interspecies differences with the human and mouse AHR C-terminal-region sequences sharing only 58% amino acid sequence identity. Compared to the mouse AHR (mAHR), the human AHR (hAHR) displays ~ 10-fold lower relative affinity for prototypical AHR ligands such as 2,3,7,8-tetrachlorodibenzo-*p*-dioxin, which has been attributed to the amino acid residue valine 381 (alanine 375 in the mAHR) in the ligand binding domain of the hAHR. We investigated whether the 10-fold difference in ligand-binding affinity between the mAHR and hAHR would be observed with a diverse range of AHR ligands. To test this hypothesis ligand binding assays were performed using the photo-affinity ligand 2-azido-3-[^{125}I]iodo-7,8-dibromodibenzo-*p*-dioxin and liver cytosol isolated from hepatocyte-specific transgenic hAHR mice and C57BL/6J mice. Remarkably, competitive ligand-binding assays revealed that, compared to the mAHR, the hAHR has a higher relative affinity for certain compounds including indirubin ((2Z) 2,3-biindole-2,3 (1´H,1´H)-dione and quercetin (2-(3,4dihydroxyphenyl)-3,5,7-trihydroxy-4H-chromen-4-one). Electro-mobility shift assays (EMSA) revealed that indirubin was more efficient at transforming the hAHR compared to the mAHR. Indirubin was also a more potent inducer of *Cyp1a1* expression in transgenic hAHR mouse hepatocytes compared to C57BL/6J mouse hepatocytes. These observations suggest that indirubin is a potent hAHR ligand that is able to selectively bind to and activate the hAHR. These discoveries imply that there may be a significant degree of structural divergence between mAHR and hAHR ligands and highlights the importance of the hAHR transgenic mouse as a model to study the hAHR *in vivo*.

Molecular Pharmacology Fast Forward. Published on March 19, 2009 as DOI: 10.1124/mol.109.054825
This article has not been copyedited and formatted. The final version may differ from this version.

The Aryl-hydrocarbon receptor (AHR) is the only ligand activated member of the basic-helix-loop-helix Per Arnt Sim (bHLH-PAS) domain family of transcription factors. Studies in *Ahr* null mice have highlighted the physiological roles of the AHR in liver and cardiac vascularization and development, immune system function and ovarian follicle maturation (Abbott et al., 1999; Fernandez-Salguero, 1995; Schmidt et al., 1996). The AHR forms a cytoplasmic complex consisting of the heat-shock protein 90 (HSP90), Hepatitis B Virus-X associated protein 2 (XAP2/AIP/ARA 9) and p23. AHR activation leads to concomitant AHR dissociation from the cytoplasmic complex and heterodimerization with the AHR nuclear translocator (ARNT). AHR/ARNT complexes bind to canonical dioxin responsive elements (DREs) and directly activate expression of a number genes including *CYP1A1, CYP1A2, CYP1B1, glutathione-S-transferase Ya, UDP-glucuronosyltransferase*, *epiregulin* and *slug* (Kohle and Bock, 2007; Qiang M. et al., 1995).

A myriad of structurally diverse compounds are known to activate the AHR through fitting into a receptor binding pocket with a maximal dimension of 14 x 12 x 5 Å (Waller and McKinney, 1995). AHR ligands are characteristically planar, aromatic and hydrophobic molecules, including polycyclic aromatic hydrocarbons (PAHs) such as benzo[*a*]pyrene (B[*a*]P), halogenated aromatic hydrocarbons (HAHs) such as 2,3,7,8-tetrachlorodibenzo-*p*-dioxin (TCDD), the hemoglobin breakdown compounds biliverdin and bilirubin, as well as a number of naturally occurring flavonols including quercetin and kaempferal (Ciolino et al., 1999; Denison and Heath-Pagliuso, 2003).

There are substantial differences in dioxin responsiveness among various mice strains, which express structurally divergent mouse AHRs (mAHR). In various inbred mice strains the $Ahr^{b1\text{-}3}$ and Ahr^{d} alleles are present. AHR expressed by the $Ahr^{b1\text{-}3}$ alleles exhibit higher affinity for dioxin, compared with AHR expressed from the Ahr^{d} allele (Poland and Glover, 1990). The

Molecular Pharmacology Fast Forward. Published on March 19, 2009 as DOI: 10.1124/mol.109.054825
This article has not been copyedited and formatted. The final version may differ from this version.

human AHR (hAHR) ligand binding domain is most structurally analogous to the mAHR^{d} allele ligand binding domain and therefore has approximately 10-fold lower affinity than the mAHR^{b} allele for TCDD, which has been attributed to the amino acid residue valine 381 (375 in mAHR) in the ligand binding domain of the hAHR (Ema et al., 1994; Harper et al., 1988; Ramadoss and Perdew, 2004).

A number of structural differences exist between the mAHR and hAHR proteins. The human and mouse AHR share only 58% amino acid sequence identity in the C-terminal half, which is the region that contains the transactivation domain (TAD) of both receptors. Interestingly, the hAHR and mAHR^{b} display distinct affinity for LXXLL-coactivator-binding motif, suggesting each receptor may differentially recruit coactivators and thus may regulate unique subsets of genes (Flaveny et al., 2008). Rodents exposed to the prototypical AHR ligand (TCDD) display a number of symptoms, including thymic atrophy, immunotoxicity, tumor promotion, teratogenicity, reproductive toxicity, hepatotoxicity and chloracne, whereas human exposure to TCDD primarily causes chloracne (Abbott et al., 1999; Connor and Aylward, 2006). Toxicity studies conducted in the human AHR "knock-in" mouse showed that TCDD-mediated toxicity differed between transgenic human *AHR* and murine *Ahr*^{d} mice, suggesting that indeed the hAHR may differ in its ability to regulate gene expression (Moriguchi et al., 2003). In addition, previous investigations have also demonstrated that the only hAHR, can be selectively activated by omeprazole through a yet to be understood mechanism that is independent of ligand binding (Lesca et al., 1995).

In light of the interspecies differences between the hAHR and the mAHR that have thus been elucidated, traditional toxicological and gene regulation studies utilizing C57BL/6J mice may be an inadequate tool for investigating the role of the hAHR in mediating toxicity and regulating gene expression. To address this issue, we developed a transgenic mouse that

Molecular Pharmacology Fast Forward. Published on March 19, 2009 as DOI: 10.1124/mol.109.054825
This article has not been copyedited and formatted. The final version may differ from this version.

expresses hAHR under the control of the liver-specific transthyretin (Ttr) promoter. Protein blot analysis has revealed that hAHR protein expression levels in the liver were similar to C57BL/6J AHR^{b} receptor levels. These transgenic *AHR^{Ttr}Ahr$^{b/b}$* mice were bred onto both the *Ahr* null mice (*Ahr* $^{-/-}$) and the albumin promoter driven *Cre* recombinase, *Ahr* floxed conditional knockout mice (*Cre^{Alb}Ahr$^{fx/fx}$*) backgrounds. Using competitive ligand binding experiments, we found that the hAHR displays a higher relative affinity for certain AHR ligands such as indirubin and quercetin compared to the mAHR^{b}, thus establishing that each receptor has distinct ligand binding characteristics. Indirubin was shown to be more potent at inducing AHR-target genes, in primary mouse hepatocytes expressing the hAHR, compared to C57BL/6J mouse hepatocytes expressing mAHR^{b}. These discoveries suggest that the hAHR may be distinctly regulated in a species-specific fashion by certain ligands, in a manner that cannot be predicted by its relatively lower affinity for prototypic AHR ligands, such as TCDD.

Molecular Pharmacology Fast Forward. Published on March 19, 2009 as DOI: 10.1124/mol.109.054825
This article has not been copyedited and formatted. The final version may differ from this version.

Materials and Methods

Transgenic mice

The synthetic human *AHR* cDNA sequence optimized for mammalian codon usage and minimal secondary mRNA structure was purchased from GenScript (Piscataway, NJ). The cDNA was amplified by PCR using primers designed with Stu I sites and the resulting product was digested with Stu I and inserted into the second exon of the modified pTTR1 vector (obtained from Dr Terry Van Dyke, University of North Carolina) (Yan et al., 1990): TTRexV3. TTRexV3 was derived by making several point mutations in the first and second exons, which destroy ATGs and introduce unique cloning sites. The TTRexV3-hAHR was digested with HIND III to release the appropriate fragment and purified for microinjection into embryos. TTRexV3-hAHR (AHR^{Ttr}) fragments were micro-injected into C57BL/6J fertilized eggs at the Penn State University Transgenic Mouse Facility (Department of Dairy and Animal Science, The Pennsylvania State University, University Park, PA). Founder mice and offspring were screened using PCR assays described below. Transgenic mice were mated with $Ahr^{-/-}$ and the albumin promoter-driven, *Cre* recombinase-expressing $Cre^{Alb}Ahr^{fx/fx}$ mice (obtained from Christopher Bradfield, University of Wisconsin) to produce transgenic $AHR^{Ttr}Ahr^{-/-}$ (strain name; B6.Cg-Ahr^{tm1Bra} Tg (Ttr-AHR)1Ghp) and $AHR^{Ttr}Cre^{Alb}Ahr^{fx/fx}$ (strain name: B6.Cg-$Ahr^{tm3.1Bra}$ Tg (Alb-cre, Ttr-AHR)1Ghp) respectively. We then used the $AHR^{Ttr}Ahr^{-/-}$ and $AHR^{Ttr}Cre^{Alb}Ahr^{fx/fx}$ mice for ligand binding experiments and gene expression analysis, respectively.

Screening of transgenic mice. Mouse tail and hepatocyte DNA was isolated using the Wizard SV Genomic DNA isolation system (Promega) and subjected to PCR using the primers for the AHR^{Ttr}, Cre^{Alb}, $Ahr^{-/-}$ genes. Analysis of $Ahr^{fx/fx}$ excision was assessed as described previously using the primers OL4062 and OL4064 in combination with the reverse primer

Molecular Pharmacology Fast Forward. Published on March 19, 2009 as DOI: 10.1124/mol.109.054825
This article has not been copyedited and formatted. The final version may differ from this version.

OL4088 (Walisser et al., 2005). The Ahr^{fxfx}-excised allele (OL4062/4088) amplified a 180-bp band, whereas amplification from the $Ahr^{fx/fx}$-unexcised allele (OL4064/4088) resulted in a 140-bp band. The Ahr^{b} allele generated a 106-bp band (OL4064/OL4088). Congenic Ahr^{d} mice were purchased from Jackson Laboratory. All mice were housed on corncob bedding at 70 ± 2°F with a 12-h light/dark cycle. Mice were given access to food and water *ad libitum*. All primer sequences are listed in Table S1.

Ligand Binding Assays

Photoaffinity ligand synthesis. The AHR photo-affinity ligand; azido-3-[^{125}I]iodo-7,8-dibromodibenzo-*p*-dioxin (PAL) was synthesized as described previously (Poland et al., 1986).

Cytosol preparation. To generate liver cytosol for ligand binding experiments mouse livers were homogenized in MENG buffer (25 mM MOPS, 2 mM EDTA, 0.02% NaN_3, 10% glycerol pH 7.4) containing 20mM sodium molybdate and protease inhibitors (Sigma) and centrifuged at 100, 000 × g for 1h.

Ligand binding conditions. All binding experiments were conducted in the dark until UV-mediated activation of the PAL. Briefly, ligand-treated lysates were incubated at room temperature (except for binding assays involving the mAHR^{d}, which was carried out at 4°C) for 20 min then photolyzed at 8 cm with 402 nm UV light. 1% dextran coated charcoal was added to the photolyzed samples which were then centrifuged at 3000 × g for 10 min to remove free ligand. Labeled samples were resolved using 8% acrylamide-TSDS-PAGE, transferred to PVDF membrane and visualized using autoradiography. Labeled AHR bands were excised and counted using a γ-counter.

Molecular Pharmacology Fast Forward. Published on March 19, 2009 as DOI: 10.1124/mol.109.054825
This article has not been copyedited and formatted. The final version may differ from this version.

Competitive binding experiments. A saturating amount of the PAL (0.21 pmol i.e.: 8×10^5 cpm per tube) was added to 150 μg total protein of mouse liver or transiently transfected COS-1 cytosol along with increasing amounts of competing ligands; benzo-[*a*]-pyrene (B[*a*]P), (2Z) 2,3-biindole-2,3 (1´H,1´H)-dione (indirubin) 2-(3,4-dihydroxyphenyl)-3,5,7-trihydroxy-4H-chromen-4-one (quercetin) 3,3',4,4',5-pentachlorobiphenyl (PCB-126) 5,6-benzoflavone (β-naphthoflavone), 5,7-dimethoxyflavone and 3-[2-(2-phenylethyl)benzoimidazole-4-yl]-3-hydroxypropanoic acid (M50354). Samples were then subjected to ligand binding conditions.

Immunoblotting

Whole mouse liver and transiently transfected COS-1 cell cytosol isolated as described above, and *in vitro*-translated rabbit reticulocyte lysate protein (50 μg/well) were resolved using 8% SDS-tricine polyacrylamide gels. Proteins were transferred to PVDF membrane and AHR protein was detected using the mouse monoclonal antibody RPT1 (Affinity BioReagents), goat anti-mouse biotin-conjugated secondary antibody and I^{125}- streptavidin and visualized using autoradiography.

Plasmids

pCI-hAHR, pCI-hAHRV381A, pcDNA3-mAHR and pcDNA3-mAHRA375V the mAHR-N-terminus/hAHR-C-terminus (m-hAHR) and hAHR-N-terminus/mAHR-C-terminus (h-mAHR) chimeric plasmid constructs were generated previously (Meyer et al., 1998; Ramadoss and Perdew, 2004).

Molecular Pharmacology Fast Forward. Published on March 19, 2009 as DOI: 10.1124/mol.109.054825
This article has not been copyedited and formatted. The final version may differ from this version.

Cell culture

COS-1 cells were routinely grown in αMEM (Sigma), supplemented with 10% fetal bovine serum (FBS), 100 IU/ml of pencillin and 100 μg/ml streptomycin.
All cell cultures were maintained under standard conditions in a 37°C incubator at 5% CO_2, 95% air and cell culture media was changed every 48 h unless otherwise indicated.

Transient transfections

COS-1 cells (ATCC, Manassas VA.) were seeded in 20 mm tissue culture plates 24 h prior to transfection, and were transfected with 20 μg of either pCI-hAhR, pCI-hAHRV381A, pcDNA3-mAhR or pcDNA3-mAHRA375V, h-mAHR and m-hAHR using LipofectAMINE reagent (Invitrogen, Carlsbad, CA), according to manufacturer's instructions.

Primary hepatocyte isolation.

Liver perfusion and hepatocyte isolation was carried out as described previously (Madden et al., 2000) with some modifications. Briefly, mice were anaesthetized with 0.1-0.3 ml 2.5% Avertin administered via intraperitoneal injection. Hepatic perfusion was performed with Buffer-I (5 mM dextrose/116 mM NaCl/760 μM NaH_2PO_4/5.3 mM KCl/26 mM $NaHCO_3$/10 mM HEPES/500 μM EGTA pH 7.2) for 1 min followed by Buffer-II (0.2 mg/ml type-I collagenase (Worthington)/ 5.3 mM KCl/116 mM NaCl/5 mM dextrose/26 mM $NaHCO_3$/1.6 mM $MgSO_4$/900 μM $CaCl_2$/48 μg/ml trypsin inhibitor pH 7.2) for a further 5-10 min. Hepatic tissue was excised, transferred and dissociated in a 100 mm plate containing 9 ml short term

Molecular Pharmacology Fast Forward. Published on March 19, 2009 as DOI: 10.1124/mol.109.054825
This article has not been copyedited and formatted. The final version may differ from this version.

media (DMEM/10% FBS/2.5% DMSO/10 nM dexamethasone,100 IU/ml penicillin/100 μg/ml streptomycin). Cells were filtered, centrifuged (500 x *g* for 1 min) and resuspended in short-term media. Cell viability was assessed via trypan blue staining and cells seeded into type-I collagen-coated 6-well plates (BD Bioscience) at a density of 1 x 10^6 cells/ml. After 4 h incubation at 37°C, non-adherent cells were aspirated and fresh short-term media added. After overnight incubation at 37°C, cells were washed with PBS and short-term media replaced with long-term hepatocyte culture media (Hepatozyme-SFM (Invitrogen)/2.5% DMSO/10 nM dexamethasone/100 IU/ml penicillin and 100 μg/ml streptomycin).

Real-time RT-PCR

Primary hepatocytes isolated from $AHR^{Ttr}Cre^{Alb}Ahr^{fx/fx}$, $Ahr^{fx/fx}$, and $Ahr^{b/b}$ mice were treated with AHR ligands (TCDD or indirubin) or vehicle control for 6 h. Total mRNA was isolated from cultured hepatocytes using Tri-reagent (Invitrogen). RNA was then converted to cDNA using ABI cDNA archive synthesis kit (ABI) and mRNA expression was quantified using real-time RT-PCR using primers listed in table S1.

Electro-Mobility Shift Assays

pCI-ARNT, pCI-hAHR, pCI-hAHRV381A, pcDNA3-mAHR and mAHRA375V along with control plasmids were *in vitro* translated using the TNT®-coupled rabbit reticulocyte lysate system(Promega) in the presence of 1.5 mM sodium molybdate. I*n vitro* translated AHR proteins (4 μL of lysate) were incubated with ARNT (4 μL of lysate) plus 1.5 μl HEDG buffer (25 mM HEPES, 1 mM EDTA 10 mM Sodium molybdate and 10% v/v glycerol pH 7.5) along with

Molecular Pharmacology Fast Forward. Published on March 19, 2009 as DOI: 10.1124/mol.109.054825
This article has not been copyedited and formatted. The final version may differ from this version.

either 10 nM B[*a*]P, 100 nM or 1 μM indirubin or vehicle control for 15 min at room temperature. P^{32}-labeled DRE probe was added to each reaction and incubated for 15 min. A total of 16 μL of lysate was then resolved using a 6% DNA-retardation gel (Invitrogen), which was then fixed, vacuum dried and visualized using autoradiography. Band intensities were quantified using a phosphorimager and OptiQuant software (Packard), and presented as digitized light units (DLU).

Statistical analysis

Statistical analysis of real-time RT-PCR data was performed using two-way ANOVA using GraphPad Prism software (GraphPad Software Inc. San Diego, CA). Calculated *p* values <0.05 were considered statistically significant.

Molecular Pharmacology Fast Forward. Published on March 19, 2009 as DOI: 10.1124/mol.109.054825
This article has not been copyedited and formatted. The final version may differ from this version.

Results

The liver-specific transgenic hAHR mouse expresses functional hAHR protein in the liver and hepatocytes at comparable levels to mAHR^{b}. In order to study the possible unique roles of the hAHR in gene regulation, toxicity and carcinogenesis in the liver, we generated a liver-specific transgenic hAHR expressing mouse. hAHR expressing mice were generated initially on a C57BL/6J background and subsequently crossed with *Ahr* $^{-/-}$ or *Cre*^{Alb}*Ahr*$^{fx/fx}$ mice to transfer the hAHR transgene to an *Ahr* null and conditional deletion background. Three *AHR*^{Ttr} transgenic mouse lines were generated that expressed differing amounts of hAHR (Fig. 1A). In transgenic mouse-line B, hAHR protein expression levels in whole liver and hepatocytes, were comparable (approximately 2-fold higher) to AHR^{b} expression in C57BL/6J mouse liver and hepatocytes (Fig. 1A and D). Liver cytosol from *AHR*^{Ttr} *Ahr*$^{-/-}$ mice was used in saturation and competitive ligand binding studies (Fig. 1B, and 2). An assessment of the binding capacity of the hAHR protein expressed in *AHR*^{Ttr}*Ahr*$^{-/-}$ transgenic mice showed that the mAHR^{b} had a higher relative ligand binding capacity for the PAL compared to the hAHR (Fig. 1B), a result consistent with previous studies (Ramadoss and Perdew, 2004).

Interestingly, the hAHR displayed high levels of constitutive activity and reduced relative inducibility of the AHR responsive genes C*yp1a1, Cyp1a2* and *Cyp1b1* when expressed on an *Ahr* $^{-/-}$ background (Fig. S1) this result was not observed in *AHR*^{Ttr}*Cre*^{Alb}*Ahr*$^{fx/fx}$ mice, which were on a *Cre*^{Alb}*Ahr*$^{fx/fx}$ background. Therefore, in order study hAHR-mediated gene regulation hepatocytes isolated from *AHR*^{Ttr}*Cre*^{Alb}*Ahr*$^{fx/fx}$ mice were used. Hepatocyte and tail clip DNA collected from transgenic mice was subjected to PCR genotyping with primers specific for the *AHR*^{Ttr} and *Cre*^{Alb} transgenes and floxed *Ahr*$^{fx/fx}$ primers to confirm *Ahr*$^{fx/fx}$ gene excision in *Cre*^{Alb} positive mice (Fig. 1C). Whole-liver and hepatocyte cytosol isolated from, *AHR*^{Ttr}*Ahr*$^{-/-}$,

Molecular Pharmacology Fast Forward. Published on March 19, 2009 as DOI: 10.1124/mol.109.054825
This article has not been copyedited and formatted. The final version may differ from this version.

AHR^{Ttr}*Cre*^{Alb}*Ahr*$^{fx/fx}$, *Ahr*$^{fx/fx}$ as well as *Ahr*$^{d/d}$ congenic and C57BL/6J mice were also all subjected to protein blot analysis (Fig. 1A-D). TCDD was able to induce *Cyp1a1* and *Cyp1b1* mRNA expression in both mAHR^{b} and hAHR expressing hepatocytes in a dose-dependent manner. TCDD at lower doses also demonstrated a notably more potent induction of *Cyp1a1* and *Cyp1b1* in mAHR^{b} expressing, compared to hAHR expressing, hepatocytes (0.1 nM-1 nM) (Fig. 1E).

The hAHR and mAHR^{b} display varied relative ligand binding affinities in competitive ligand binding assays. The most commonly utilized mouse AHR allele in gene expression, toxicity and carcinogenesis studies is the mAHR^{b} allele. We used this allele to compare ligand binding characteristics of the human and mouse Ah receptors for a structurally diverse subset of AHR ligands (Fig. 2). Liver cytosol isolated from both mAHR^{b} and hAHR transgenic mice were subjected to competitive ligand binding assays using a fixed saturating dose of PAL (0.21 pmol i.e.: 8×10^5 cpm per tube) and increasing amounts of known AHR ligands. These competition binding experiments showed that compared to the hAHR the mAHR had a higher relative affinity for the competing ligands B[*a*]P, β-naphthoflavone and PCB-126 (~10-fold) relative to the PAL (Fig. 3A). Relative to the PAL, the hAHR displayed a reduced but still lower relative-ligand binding affinity for 5, 7-dimethoxyflavone and M50354 compared to the mAHR (Fig. 3B). Surprisingly, the hAHR displayed a higher relative-affinity for quercetin and the plant tryptophan derivative indirubin compared to the mAHR (Fig. 3C). Taken together this data suggests that the human and mouse AHR ligand binding pocket has differential binding properties.

Indirubin more potently induces hAHR transformation compared to the mAHR. Ligand binding converts the AHR to a high affinity DNA binding form which is comprised of an AHR/ARNT heterodimer; a process known as transformation. We decided to investigate whether

Molecular Pharmacology Fast Forward. Published on March 19, 2009 as DOI: 10.1124/mol.109.054825
This article has not been copyedited and formatted. The final version may differ from this version.

the higher relative affinity the hAHR displayed for indirubin and quercetin in competitive binding experiments would also result in selective transformation of the hAHR by these compounds. EMSAs showed that indirubin was able to more potently induce hAHR heterodimerization and DRE binding compared to the mAHR^{b} (Fig. 4A-B). Notably, compared to B[*a*]P, indirubin was also relatively more effective at inducing hAHR transformation for all the concentrations at which both ligands were tested (Fig. 4A). Interestingly, although quercetin was unable to induce profound mAHR or hAHR transformation, quercetin was able to transform the hAHR at lower ligand concentrations (as low as 1 μM) which failed to stimulate mAHR transformation (Fig. 4A).

Indirubin is more potent at stimulating hAHR driven gene activation. In order to test whether indirubin was able to selectively activate the hAHR, primary hepatocytes isolated from mAHR^{b} and hAHR mice were treated with increasing doses of indirubin and assayed for AHR responsive gene induction using real-time RT-PCR. At lower doses, indirubin selectively induced *Cyp1a1* mRNA synthesis only in hAHR expressing hepatocytes. At higher doses, indirubin also differentially increased *Cyp1b1* mRNA levels in hAHR expressing hepatocytes compared to mAHR hepatocytes (Fig. 4C).

hAHR relative affinity for indirubin is not enhanced by V381A substitution. The mAHR^{d} has a ligand binding domain that is analogous to that of the hAHR and thus has an ~ 10 fold lower affinity than the mAHR^{b}, but only a ~2-fold higher affinity compared to the hAHR for typical AHR ligands like TCDD (Poland and Glover, 1990; Ramadoss and Perdew, 2004). Previous investigations have demonstrated that the low relative ligand binding affinity displayed by the hAHR and mAHR^{d} is due to a valine at residue 381 in the hAHR and 375 in mAHR^{d}. Substituting valine 381 with an alanine residue (hAHR-V381A) has therefore been shown to enhance the relative ligand binding affinity of the hAHR to equal that of the mAHR^{b} and

Molecular Pharmacology Fast Forward. Published on March 19, 2009 as DOI: 10.1124/mol.109.054825
This article has not been copyedited and formatted. The final version may differ from this version.

enhanced photoaffinity ligand binding capacity (Ema et al., 1994; Ramadoss and Perdew, 2004). Since the mAHR^{d} is thermally unstable at room temperature (Poland and Glover, 1990), the thermally stable yet binding deficient low affinity mAHR^{b} point mutant in which alanine 375 is substituted by valine (mAHR-A375V), was instead used in competitive ligand binding experiments. To find out if indeed valine 381 was responsible for the higher relative affinity the hAHR displayed for indirubin, competitive ligand binding assays were conducted using increasing doses of indirubin and cytosol isolated from Cos-1 cells transiently transfected with either, hAHR, hAHR-V381A, mAHR, or mAHR-A375V constructs. The level of expression of each receptor was similar (Fig. 5C). Surprisingly, compared to the hAHR, the V381A substitution slightly reduced the relative ligand binding affinity of the hAHR for indirubin (Fig. 5A). In contrast, the mAHR-A375V mutation did not significantly alter the difference in relative binding affinity between the low affinity mAHR-A375V and high affinity mAHR for indirubin, relative to the PAL.

The C-terminal transactivation domain of the hAHR and mAHR does not affect the relative affinity of each receptor for indirubin. Cos-1 cells were transiently transfected with the chimeric constructs h-mAHR and m-hAHR. These chimeric receptors have the C-terminal domains swapped as previously described (Ramadoss and Perdew, 2005). These receptors were used to investigate whether differences between the human and mouse receptor transactivation domains or three dimensional folding of the receptors may have contributed to the observed differences in relative ligand binding affinities between the mAHR and hAHR. Competitive ligand binding assays with indirubin involving the hAHR and mAHR protein chimeras h-mAHR and m-hAHR, showed no difference in the relative ligand binding affinities when compared to that observed with the full length hAHR and mAHR respectively (Fig. 5B and 3C). The level of chimeric receptor expression was similar in the cytosol used for ligand binding (Fig. 5C). These

Molecular Pharmacology Fast Forward. Published on March 19, 2009 as DOI: 10.1124/mol.109.054825
This article has not been copyedited and formatted. The final version may differ from this version.

results indicate that the C-terminal transactivation domain does not modulate ligand binding affinity.

Transformation of hAHR by indirubin is disrupted by V381A substitution. In order to elucidate whether V381 or A375 is critical for efficient indirubin stimulated transformation of hAHR and mAHR, respectively, EMSAs were performed using in vitro translated hAHR, hAHR-V381A, mAHR and mAHR-A375V. For the mAHR, the A375V substitution reduced mAHR transformation in response to indirubin (Fig. 6A and C). Surprisingly, for the hAHR, the V381A substitution also reduced (~2-fold) the efficiency of indirubin mediated receptor transformation (Fig. 6B-C). Suggesting that the presence of the valine residue at position 381 does not reduce hAHR receptor affinity for indirubin, yet does decrease B[*a*]P binding and subsequent transformation.

Molecular Pharmacology Fast Forward. Published on March 19, 2009 as DOI: 10.1124/mol.109.054825
This article has not been copyedited and formatted. The final version may differ from this version.

Discussion

Historically, studies aimed at examining the physiological function of the AHR, as well as its role in mediating PAH/HAH-driven toxicity and carcinogenesis, have utilized rodent models, with the expectation that the data can be extrapolated to humans. The hAHR has a 10-fold lower affinity for typical AHR ligands like TCDD compared to the most studied mAHR^{b} allele. However, a number of recent investigations have demonstrated that the hAHR may possess a significant number of contrasting properties compared with the mAHR, which may limit the reliability of using rodent model systems to predict hAHR function. High homology of the hAHR to the guinea pig AHR; the rodent most sensitive to TCDD, suggested that humans might also be highly responsive to TCDD (Korkalainen et al., 2001). In addition, examination of hAHR ligand specificity compared with those of zebrafish and rainbow trout AHRs revealed that mono-ortho polychlorinated biphenyls activated hAHR but were not very effective in activating either zebrafish or rainbow trout AHRs (Abnet et al., 1999), suggesting that the hAHR may specifically bind a structurally unique subset of ligands. Interestingly, *CYP1A1* induction in response to TCDD treatment was also shown to be most potent in human lymphocytes, as compared to mouse and rat lymphocytes (Keiko et al., 2006). Conversely, using a "knock-in" hAHR mouse Moriguchi *et al* demonstrated that the hAHR was resistant to TCDD mediated toxicity when compared to the mAHR^{d}, suggesting that indeed humans might also be resistant to TCDD-mediated toxicity. However it should be noted that, this humanized AHR mouse failed to show hAHR protein expression data, thus casting doubt on the validity of this model. Concordantly, studies that examined various toxicological endpoints in a myriad of animal models provided evidence supporting the traditional conclusion that impaired hAHR-ligand binding correlates with TCDD resistance *in vivo* (Connor and Aylward, 2006). The hAHR has

Molecular Pharmacology Fast Forward. Published on March 19, 2009 as DOI: 10.1124/mol.109.054825
This article has not been copyedited and formatted. The final version may differ from this version.

also been shown to differentially recruit coactivator-LXXLL motifs which suggests that the hAHR and mAHR may actually regulate gene expression through recruitment of distinct coactivators (Flaveny et al., 2008). In order to comprehend the physiological and toxicological role of the hAHR we developed a transgenic hAHR mouse that expresses hAHR only in the liver. Real-time RT-PCR analysis showed that the hAHR is less responsive to TCDD induced activation at lower doses compared to the mAHR^{b} in primary hepatocytes, which is consistent with numerous published studies in human cell lines. This transgenic mouse model is unique in that it allows a direct comparison of hAHR and mAHR function within the same cellular background (e.g. coactivators, response elements, etc.) in an *in vivo* system. Furthermore, the use of the *Ahr* $^{fx/fx}$/Cre^{Alb} conditional knockout system as a background on which to express the hAHR in hepatocytes permits the study of the hAHR, while circumventing the physiological problems encountered with transgenic mice where hAHR is expressed on an *Ahr* $^{-/-}$ background. For example, the isolation of hepatocytes from *Ahr* $^{-/-}$ mice is difficult, possibly due to aberrant hepatic vascularization (data not shown). In contrast, isolation of hAHR expressing hepatocytes in transgenic mice on the *Ahr* $^{fx/fx}$/Cre^{Alb} background is similar to that of C57BL/6J mice. Also, the hAHR displayed high levels of constitutive activity and limited inducibility when expressed on an *Ahr* $^{-/-}$ background (Fig. S1) which was not observed when hAHR is expressed on an *Ahr* $^{fx/fx}$/Cre^{Alb} background.

Competitive ligand binding experiments involving a number of AHR ligands highlighted that, in contrast with the mAHR, the hAHR may display high affinity to a distinct subset of ligands that are structurally divergent from typical exogenous AHR ligands like TCDD. As expected, the mAHR^{b} showed a higher relative ligand binding affinity for the AHR ligands B[*a*]P, PCB-126 and β-NF. Yet, compared to the mAHR^{b},the hAHR demonstrated a higher relative-ligand binding affinity for quercetin and indirubin specifically. Indirubin has been

Molecular Pharmacology Fast Forward. Published on March 19, 2009 as DOI: 10.1124/mol.109.054825
This article has not been copyedited and formatted. The final version may differ from this version.

shown previously to be 35-140-fold more potent at inducing hAHR than mAHR activity in a yeast reporter system (Kawanishi et al., 2003). In these competitive ligand binding studies, gene expression analysis and EMSA analysis all suggest that indirubin is a high-potency, high-affinity hAHR specific ligand. The "high-ligand-affinity" hAHR-V381A substitution in the hAHR ligand binding domain, instead partially inhibited the high-binding affinity interaction and potent transformation of the hAHR by indirubin. This was in contrast with expected observations based on previous mutagenesis analysis of the ligand binding domain of the hAHR. Illuminating the specific amino acid residues that are critical to high-affinity hAHR/indirubin interaction will require further investigation. Another possible explanation is that, despite the hAHR V381 ligand binding pocket mutation, binding of the endogenous hAHR ligand(s) is still conserved. Indeed, the hAHR ligand binding pocket may actually utilize distinct residues to stably bind to traditionally defined low affinity and high affinity ligands (Backlund and Ingelman-Sundberg, 2004). These results suggest that the hAHR ligand binding pocket may not actually be functionally impaired but instead structurally adapted to binding ligands which are in structural contrast with known high-affinity exogenous mAHR ligands. This fact has implications for future investigations aimed at discovering high-affinity endogenous hAHR ligands. Future studies therefore should take into account that potential hAHR ligands may be structurally distinct from high-affinity mAHR ligands. Furthermore, the hAHR may indeed have unique molecular properties that contrast with the mAHR, which highlight the limitations of using rodent AHRs in model systems geared toward understanding the role of the hAHR in gene regulation, toxicity and carcinogenesis. The hAHR expressing transgenic mouse lines described here may therefore be valuable for testing several hypotheses relevant to hAHR activity that may not be discerned in typical rodent models.

Molecular Pharmacology Fast Forward. Published on March 19, 2009 as DOI: 10.1124/mol.109.054825
This article has not been copyedited and formatted. The final version may differ from this version.

Acknowledgements

We thank Dr. Christopher Bradfield for kindly providing the *Ahr*$^{fx/fx}$*Cre*^{Alb} mice and helpful discussions.

References

Abbott BD, Schmid JE, Pitt JA, Buckalew AR, Wood CR, Held GA and Diliberto JJ (1999) Adverse Reproductive Outcomes in the Transgenic Ah Receptor-Deficient Mouse. *Toxicology and Applied Pharmacology* **155**:62-70.

Abnet CC, Tanguay RL, Heideman W and Peterson RE (1999) Transactivation activity of human, zebrafish, and rainbow trout aryl hydrocarbon receptors expressed in COS-7 cells: greater insight into species differences in toxic potency of polychlorinated dibenzo-*p*-dioxin, dibenzofuran, and biphenyl congeners. *Toxicol Appl Pharmacol* **159**:41-51.

Backlund M and Ingelman-Sundberg M (2004) Different structural requirements of the ligand binding domain of the aryl hydrocarbon receptor for high- and low-affinity ligand binding and receptor activation. *Mol Pharmacol* **65**:416-25.

Ciolino HP, Daschner PJ and Yeh GC (1999) Dietary flavonols quercetin and kaempferol are ligands of the aryl hydrocarbon receptor that affect CYP1A1 transcription differentially. *Biochem J* **340 (Pt 3)**:715-22.

Connor KT and Aylward LL (2006) Human response to dioxin: aryl hydrocarbon receptor (AhR) molecular structure, function, and dose-response data for enzyme induction indicate an impaired human AhR. *J Toxicol Environ Health B Crit Rev* **9**:147-71.

Denison MS and Heath-Pagliuso S (2003) The Ah receptor: A regulator of the biochemical and toxicologyical actions of structurally diverse chemicals. *Bull Environ Contam Toxicol* **61**:557-568.

Ema M, Ohe N, Suzuki M, Mimura J, Sogawa K, Ikawa S and Fujii-Kuriyama Y (1994) Dioxin binding activities of polymorphic forms of mouse and human arylhydrocarbon receptors. *J Biol Chem* **269**:27337-43.

Fernandez-Salguero PM (1995) Immune system impairment and hepatic fibrosis in mice lacking the dioxin-binding Ah receptor. *Science* **268**:722-726.

Flaveny C, Reen RK, Kusnadi A and Perdew GH (2008) The mouse and human Ah receptor differ in recognition of LXXLL motifs. *Arch Biochem Biophys.*

Harper PA, Golas CL and Okey AB (1988) Characterization of the Ah receptor and aryl hydrocarbon hydroxylase induction by 2,3,7,8-tetrachlorodibenzo-*p*-dioxin and benz(a)anthracene in the human A431 squamous cell carcinoma line. *Cancer Res* **48**:2388-95.

Kawanishi M, Sakamoto M, Ito A, Kishi K and Yagi T (2003) Construction of reporter yeasts for mouse aryl hydrocarbon receptor ligand activity. *Mutat Res* **540**:99-105.

Keiko N, Kana A, Yoshimi M, Tomohiro I, Takehiro S, Hiroyoshi T and Chiharu T (2006) Comparison of the 2,3,7,8-tetrachlorodibenzo-*p*-dioxin (TCDD)-induced CYP1A1 gene expression profile in lymphocytes from mice, rats, and humans: Most potent induction in humans. *Toxicology*:49465-49475.

Kohle C and Bock KW (2007) Coordinate regulation of phase I and II xenobiotic metabolism by the Ah receptor and Nrf2. *Biochem Pharmacol* **73**:1853-62.

Korkalainen M, Tuomisto J and Pohjanvirta R (2001) The AH Receptor of the Most Dioxin-Sensitive Species, Guinea Pig, Is Highly Homologous to the Human AH Receptor. *Biochemical and Biophysical Research Communications* **285**:1121-1129.

Lesca P, Peryt B, Larrieu G, Alvinerie M, Galtier P, Daujat M, Maurel P and Hoogenboom L (1995) Evidence for the ligand-independent activation of the AH receptor. *Biochem Biophys Res Commun* **209**:474-82.

Madden CR, Finegold MJ and Slagle BL (2000) Expression of hepatitis B virus X protein does not alter the accumulation of spontaneous mutations in transgenic mice. *J Virol* **74**:5266-72.

Meyer BK, Pray-Grant MG, Vanden Heuvel JP and Perdew GH (1998) Hepatitis B virus X-associated protein 2 is a subunit of the unliganded aryl hydrocarbon receptor core complex and exhibits transcriptional enhancer activity. *Mol Cell Biol* **18**:978-88.

Moriguchi T, Motohashi H, Hosoya T, Nakajima O, Takahashi S, Ohsako S, Aoki Y, Nishimura N, Tohyama C, Fujii-Kuriyama Y and Yamamoto M (2003) Distinct response to dioxin in an arylhydrocarbon receptor (AHR)-humanized mouse. *PNAS* **100**:5652-5657.

Poland A and Glover E (1990) Characterization and strain distribution pattern of the murine Ah receptor specified by the Ah^{d} and Ah^{b-3} alleles. *Mol Pharmacol* **38**:306-12.

Poland A, Glover E, Ebetino H and Kende A (1986) Photoaffinity labelling of the Ah receptor. *Food Chem Toxicol* **24**:781-7.

Qiang M., Dong L and Whitlock Jr. JP (1995) Transcriptional Activation by the Mouse Ah Receptor. *J. Biol. Chem.* **270**:12697-12703.

Ramadoss P and Perdew GH (2004) Use of 2-Azido-3-[^{125}I]iodo-7,8-dibromodibenzo-p-dioxin as a Probe to Determine the Relative Ligand Affinity of Human versus Mouse Aryl Hydrocarbon Receptor in Cultured Cells. *Molecular Pharmacology* **66**:129-136.

Ramadoss P and Perdew GH (2005) The transactivation domain of the Ah receptor is a key determinant of cellular localization and ligand-independent nucleocytoplasmic shuttling properties. *Biochemistry* **44**:11148-59.

Schmidt JV, Su GH-T, Reddy JK, Simon MC and Bradfield CA (1996) Characterization of a murine Ahr null allele: Involvement of the Ah receptor in hepatic growth and development 10.1073/pnas.93.13.6731. *PNAS* **93**:6731-6736.

Walisser JA, Glover E, Pande K, Liss AL and Bradfield CA (2005) Aryl hydrocarbon receptor-dependent liver development and hepatotoxicity are mediated by different cell types. *Proc Natl Acad Sci U S A* **102**:17858-63.

Waller CL and McKinney JD (1995) Three-dimensional quantitative structure-activity relationships of dioxins and dioxin-like compounds: model validation and Ah receptor characterization. *Chem Res Toxicol* **8**:847-58.

Yan C, Costa RH, Darnell JE, Jr., Chen JD and Van Dyke TA (1990) Distinct positive and negative elements control the limited hepatocyte and choroid plexus expression of transthyretin in transgenic mice. *Embo J* **9**:869-78.

Molecular Pharmacology Fast Forward. Published on March 19, 2009 as DOI: 10.1124/mol.109.054825
This article has not been copyedited and formatted. The final version may differ from this version.

Footnote:

This work was supported by NIH grant ES04869 and the Dow Chemical Company.

Molecular Pharmacology Fast Forward. Published on March 19, 2009 as DOI: 10.1124/mol.109.054825
This article has not been copyedited and formatted. The final version may differ from this version.

Legends for Figures

Fig. 1. The liver-specific transgenic hAHR mouse expresses functional hAHR protein in the liver and hepatocytes at comparable levels to mAHR^b in C57BL/6J mice. A, hAHR transgenic mice (lines A, B, C) express hAHR protein at comparable levels to mAHR^b protein expression in liver. B, Whole liver and cultured primary hepatocyte, hAHR expression in selected *AHR^{Ttr}* transgenic mouse line (line B) used in ligand binding and gene expression experiments. C, PCR genotyping of DNA isolated from tail clip and hepatocyte DNA from *Ahr$^{fx/fx}$*, *Ahr$^{fx/fx}$Cre^{Alb}* and *AHR^{Ttr}Ahr$^{fx/fx}$Cre^{Alb}* transgenic mice on a conditional knockout background was conducted using primers for *AHR^{Ttr}*, *Cre^{Alb}* and *Ahr^{fx}*. *Ahr^{fx}* excision was assessed as described previously using the primers OL4062 and OL4064 combination with the reverse primer OL4088 (Walisser et al., 2005). The *Ahr^{fx}*-excised allele amplified a 180-bp band, whereas amplification from the *Ahr^{fx}*-unexcised allele resulted in a 140-bp band. *Ahr^b* C57BL/6J allele generated a 106-bp band. D, Saturation ligand binding. Increasing amounts of PAL were added to liver cytosol isolated from the hAHR expressing transgenic line B on an *Ahr$^{fx/fx}$Cre^{Alb}* background and C57BL/6J, mAHR^b expressing mice. Labeled samples were resolved using 8% acrylamide-tricine SDS-PAGE, transferred to PVDF membrane and visualized using autoradiography. Radioactive AHR bands were excised and counted using a γ-counter. E, Real-Time RT-PCR. TCDD treated cultured primary hepatocytes isolated from *AHR^{Ttr}Ahr$^{fx/fx}$Cre^{Alb}*, *Ahr^b* mice were treated with increasing amounts of TCDD or vehicle control for 6 h. mRNA expression was quantified using real-time RT-PCR. (* $p<0.05$)

Fig. 2. AHR ligands. A structurally diverse set of AHR ligands were chosen for use in competitive ligand binding assays.

Molecular Pharmacology Fast Forward. Published on March 19, 2009 as DOI: 10.1124/mol.109.054825
This article has not been copyedited and formatted. The final version may differ from this version.

Fig. 3. The hAHR and mAHR^b displays varied relative ligand binding affinities in competitive ligand binding assays. A-C, A saturating amount of the PAL (0.21 pmol) was added to 150 μg total protein of mouse liver cytosol along with increasing amounts of competing ligands; B[*a*]P, indirubin, quercetin, β-naphthoflavone, 5,7-dimethoxyflavone and M50354. Labeled samples were resolved using 8% acrylamide-TSDS-PAGE, transferred to PVDF membrane and visualized using autoradiography. Labeled AHR bands were excised and counted using a γ-counter.

Fig. 4. Indirubin more potently induces hAHR transformation and gene activation compared to the mAHR^b**.** A-B, Electron mobility shift assays: pCI-ARNT, pCI-hAHR and pcDNA3-mAHR were *in vitro* translated. *In vitro* translated AHR proteins were incubated with ARNT plus HEDG buffer along with either 10 nM B[*a*]P, 100 nM or 1 μM indirubin or vehicle control and P^{32}-labeled DRE probe. Lysate was then resolved using a DNA-retardation gel, fixed, vacuum dried and visualized using autoradiography. Band intensities were quantified using a phosphorimager and presented as digitized light units (DLU). C, Real time RT-PCR. Primary hepatocytes isolated from hAHR, and mAHR^b expressing mice were treated with increasing amounts of indirubin or vehicle control for 6 h. Total mRNA was isolated from cultured hepatocytes and mRNA expression was quantified using real-time RT-PCR.

Fig. 5. The high ligand-affinity V381A substitution in the hAHR ligand binding domain does not enhance hAHR relative ligand binding affinity for indirubin and the hAHR C-terminal transactivation domain does not influence hAHR ligand-binding affinity for indirubin. A, V381 substitution does not enhance the relative ligand binding affinity of the hAHR for indirubin. B,

Molecular Pharmacology Fast Forward. Published on March 19, 2009 as DOI: 10.1124/mol.109.054825
This article has not been copyedited and formatted. The final version may differ from this version.

The C-terminal transactivation domain of the hAHR or mAHR does not affect the relative affinity of each receptor for indirubin. COS-1 cells were transfected with 20 μg of pCI-hAHR, pCI-hAHRV381A, pcDNA3-mAhR or pcDNA3-mAHRA375V, h-mAHR and m-hAHR using LipofectAMINE reagent. Cytosol isolation and competitive ligand binding was carried out as described previously.

Fig. 6. Transformation of hAHR by indirubin is disrupted by V381A substitution.
A-C, Electro-mobility shift assays: pCI-ARNT, pCI-hAHR, pCI-hAHRV381A, pcDNA3-mAHR^{b} and mAHRA375V were *in vitro* translated using the TNT®-coupled rabbit reticulocyte lysate system. *In vitro* translated AHR proteins were subjected to EMSA using 10 nM B[*a*]P and 0.1 μM and 1 μM indirubin and then quantified as described previously. D, Western blot of *in vitro*-translated rabbit reticulocyte lysate, protein was resolved using 8% SDS-Tricine polyacrylamide gels. Proteins were transferred to PVDF membrane and AHR protein was detected using the mouse monoclonal antibody RPT1 and visualized using autoradiography. AHR bands were quantified using a multiple purpose phosphorimager screen and OptiQuant software and presented as digitized light units (DLU). (*p<0.05)

Figure S1. The hAHR displays high levels of constitutive activity when expressed on an *Ahr*$^{-/-}$ background. Transgenic *AHR*^{Ttr} mice on an *Ahr*$^{-/-}$ background (*AHR*^{Ttr}*Ahr*$^{-/-}$), C57BL/6J (*Ahr*^{b}), and *Ahr*$^{-/-}$ mice were injected with a saturating dose of 100 μg/kg TCDD or corn oil control. After 5 h mRNA was isolated from whole liver sections and subjected RT-real time PCR analysis with primers for *Cyp1a1*, *Cyp1a2* and *Cyp1b1*.

Fig. 1

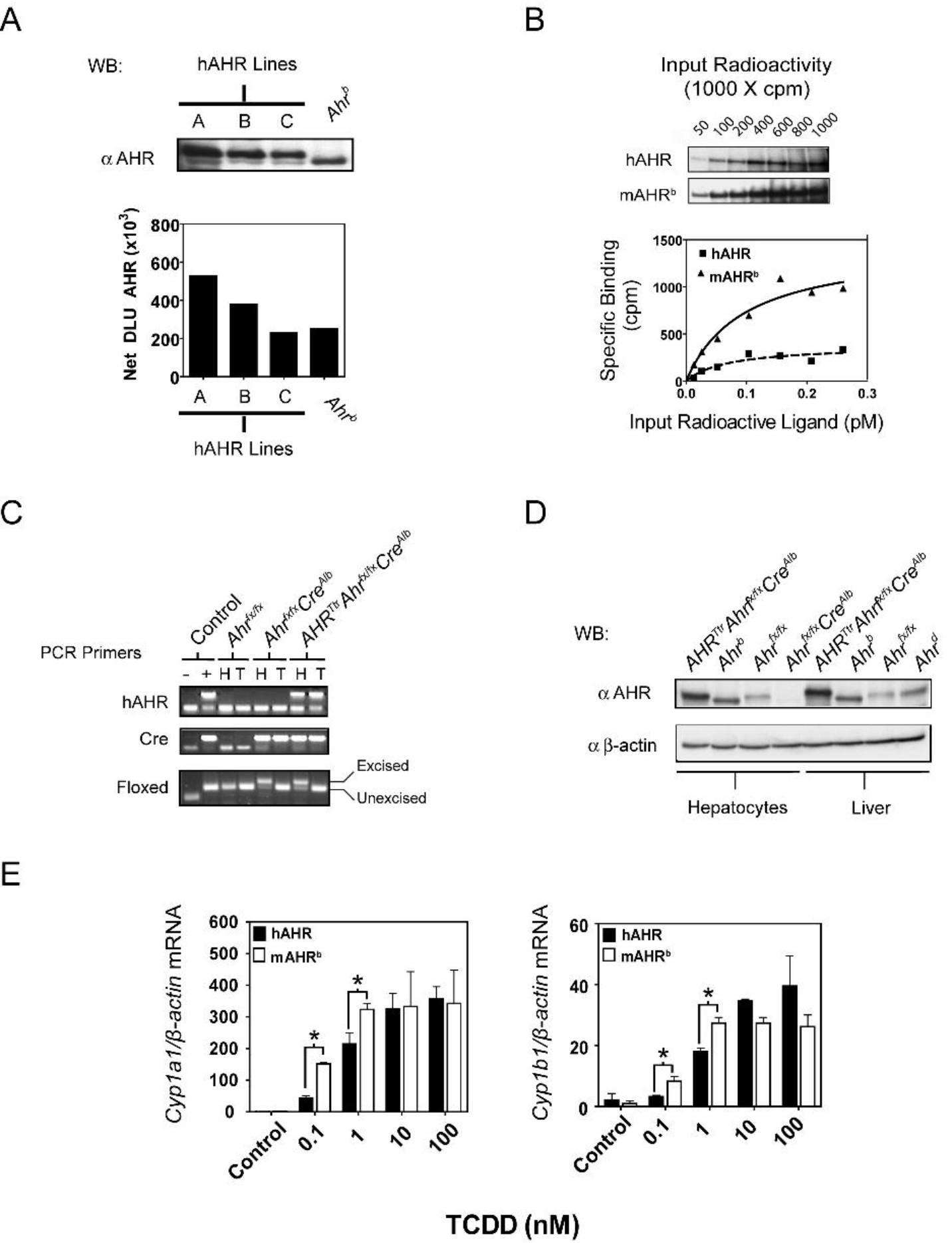
A
WB:
hAHR Lines
A
B
C
Ahrb
α AHR
Net DLU AHR (x10^3)
800
600
400
200
0
A
B
C
Ahrb
hAHR Lines
B
Input Radioactivity
(1000 X cpm)
50
100
200
400
600
800
1000
hAHR
mAHRb
Specific Binding
(cpm)
1500
1000
500
0
hAHR
mAHRb
0.0
0.1
0.2
0.3
Input Radioactive Ligand (pM)
C
Control
Ahrfx/fx
Ahrfx/fxCreAlb
AHRTtrAhrfx/fxCreAlb
PCR Primers
- + H T H T H T
hAHR
Cre
Floxed
Excised
Unexcised
D
WB:
AHRTtrAhrfx/fxCreAlb
Ahrb
Ahrfx/fx
Ahrfx/fxCreAlb
AHRTtrAhrfx/fxCreAlb
Ahrb
Ahrfx/fx
Ahrd
α AHR
α β-actin
Hepatocytes
Liver
E
Cyp1a1/β-actin mRNA
600
500
400
300
200
100
0
hAHR
mAHRb
*
*
Control
0.1
1
10
100
Cyp1b1/β-actin mRNA
60
40
20
0
hAHR
mAHRb
*
*
Control
0.1
1
10
100
TCDD (nM)

Fig. 2

Benzo-[*a*]-pyrene

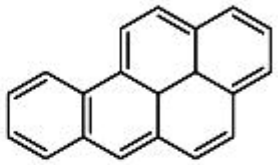

benzo-[*a*]-pyrene

β-Naphthoflavone

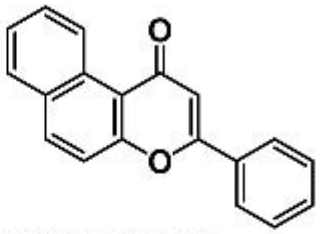

5,6-benzoflavone

5,7-Dimethoxyflavone

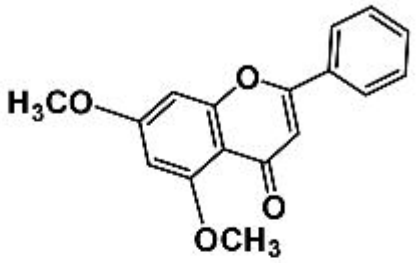

5,7-dimethoxyflavone

PCB-126

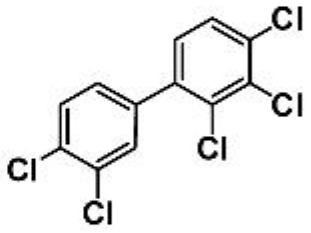

3,3',4,4',5-Pentachlorobiphenyl

Quercetin

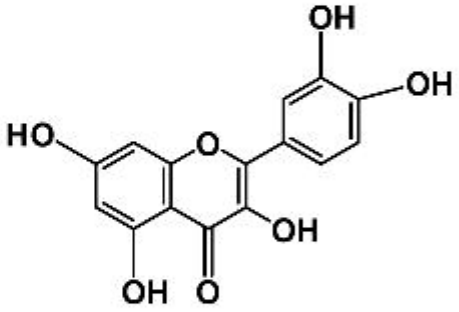

2-(3,4-dihydroxyphenyl)- 3,5,
7-trihydroxy-4H-chromen-4-one

M50354

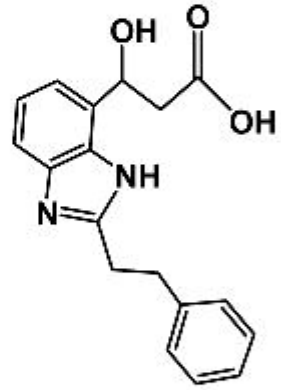

3-[2-(2-phenylethyl)benzoimidazole-
4-yl]-3-hydroxypropanoic acid

Indirubin

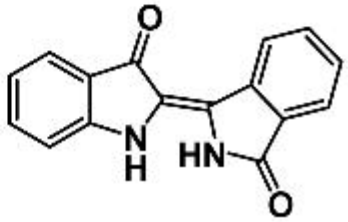

(2Z)-2,3'-biindole-2',3(1H,1'H)-dione

TCDD

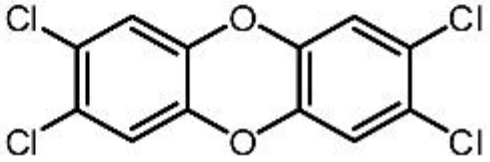

2,3,7,8 tetrachlorodibenzo-*p*-dioxin

Photo-affinity ligand

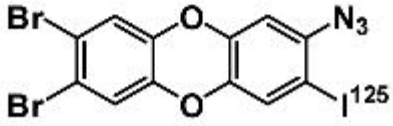

2-azido-3-[125I]iodo-7,
8-dibromodibenzo-p-dioxin

Fig. 3

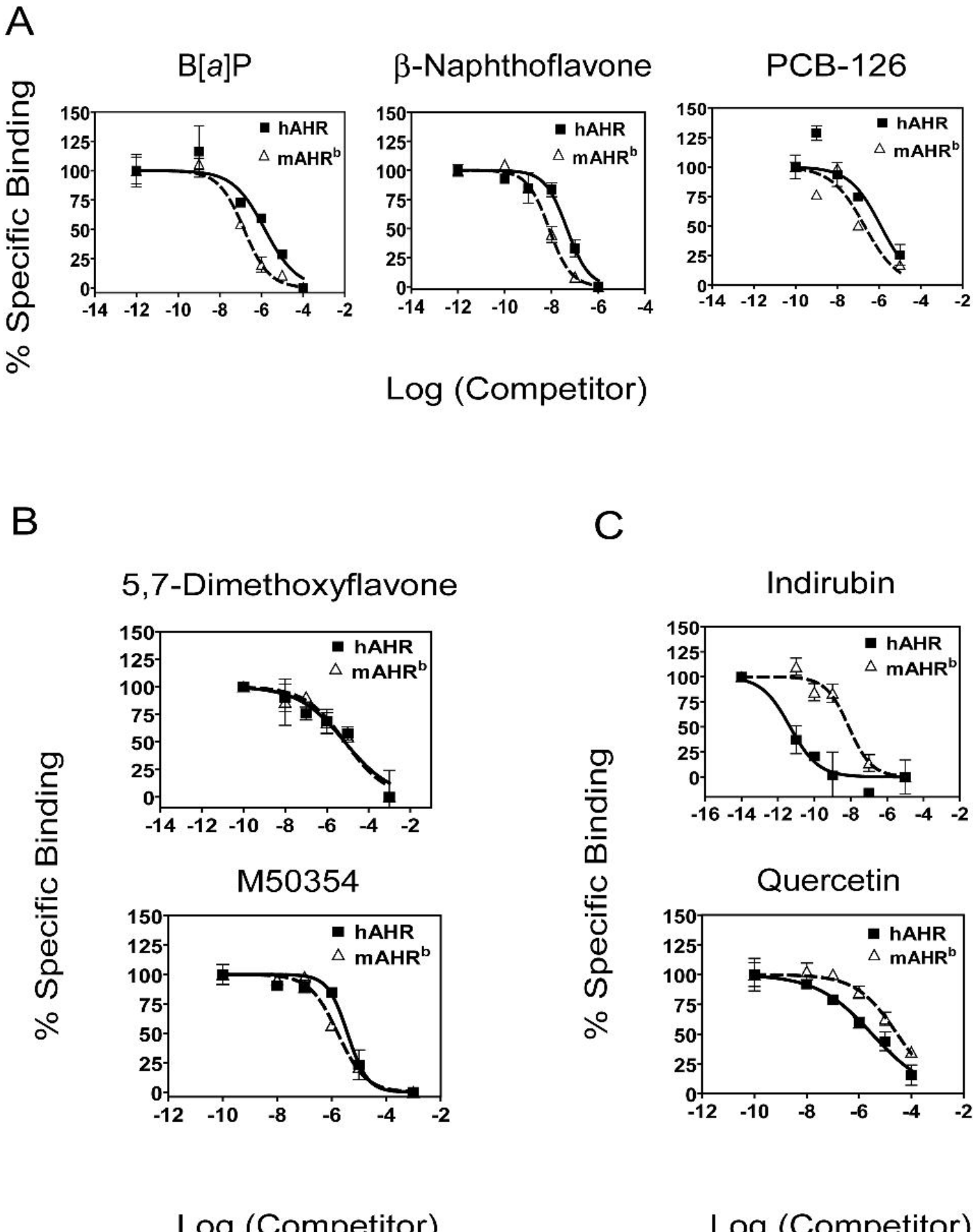
A
B[a]P
β-Naphthoflavone
PCB-126
hAHR
mAHRb
% Specific Binding
Log (Competitor)
B
5,7-Dimethoxyflavone
M50354
C
Indirubin
Quercetin

Fig. 4

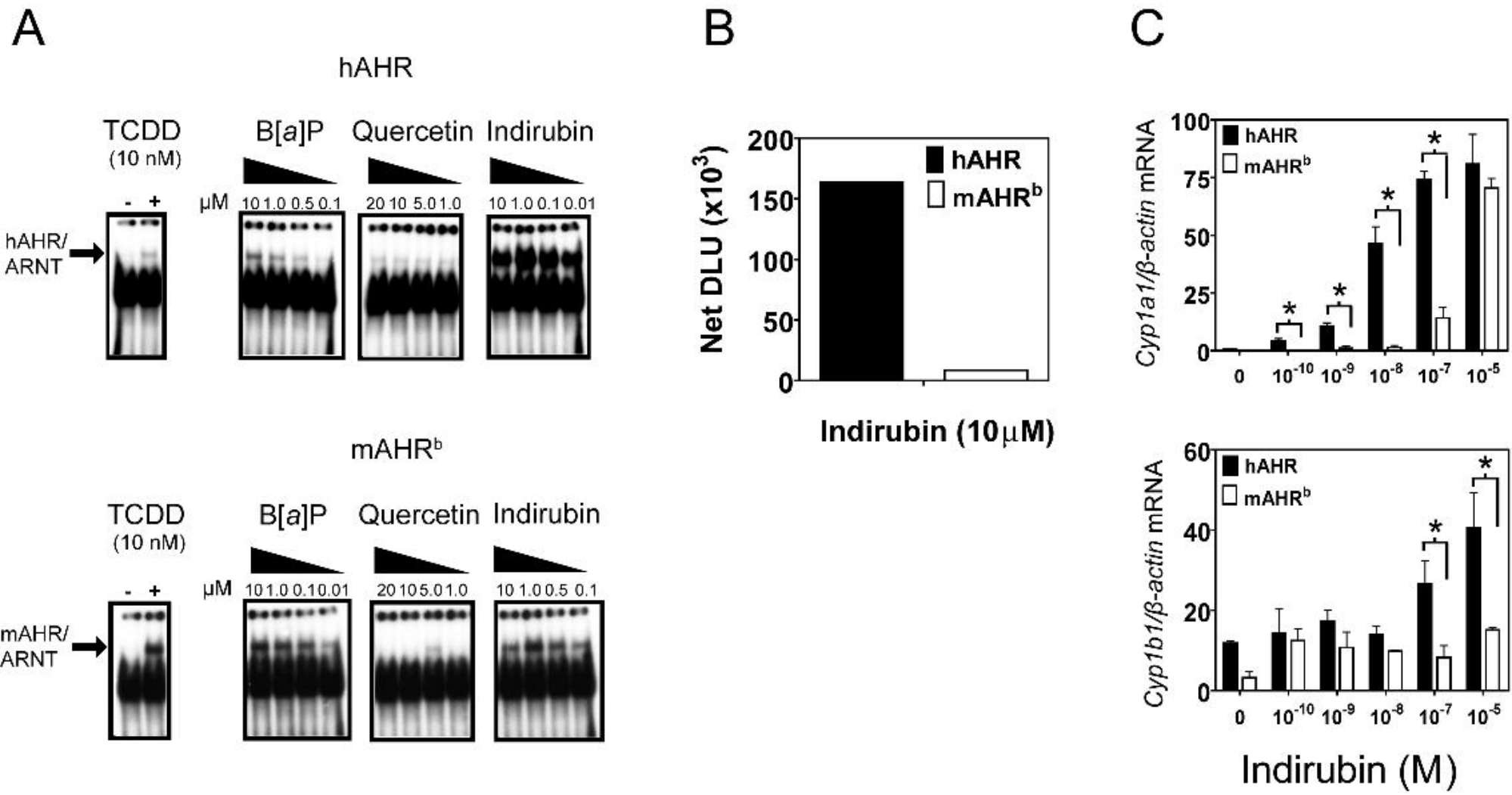
A
hAHR
TCDD
(10 nM)
B[a]P
Quercetin
Indirubin
- +
μM 10 1.0 0.5 0.1
20 10 5.0 1.0
10 1.0 0.1 0.01
hAHR/
ARNT
mAHRb
TCDD
(10 nM)
B[a]P
Quercetin
Indirubin
- +
μM 10 1.0 0.1 0.01
20 10 5.0 1.0
10 1.0 0.5 0.1
mAHR/
ARNT
B
Net DLU (x10^3)
200
150
100
50
0
hAHR
mAHRb
Indirubin (10μM)
C
Cyp1a1/β-actin mRNA
100
75
50
25
0
hAHR
mAHRb
0
10^-10
10^-9
10^-8
10^-7
10^-5
Cyp1b1/β-actin mRNA
60
40
20
0
hAHR
mAHRb
0
10^-10
10^-9
10^-8
10^-7
10^-5
Indirubin (M)

Fig. 5

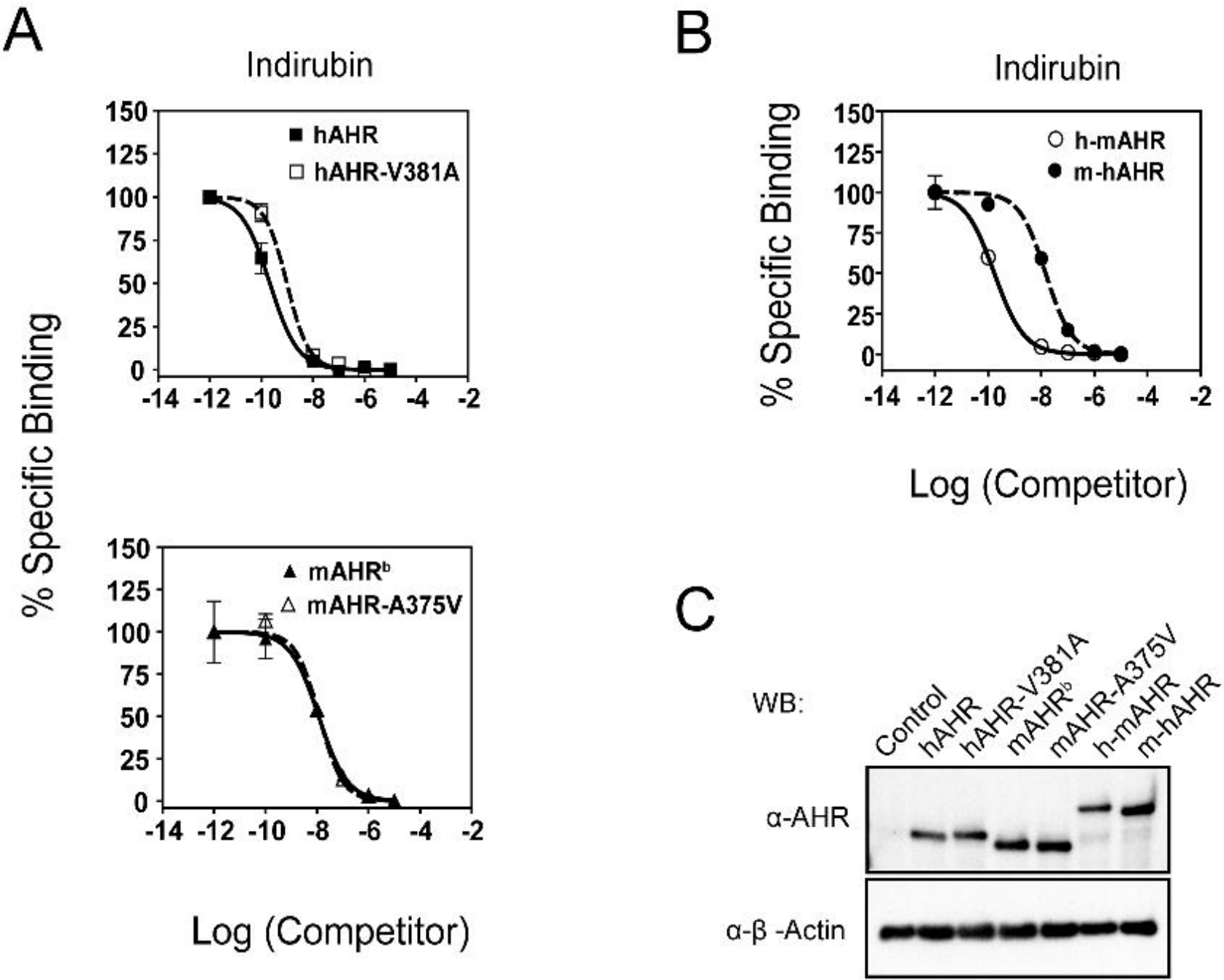
A
Indirubin
% Specific Binding
150
125
100
75
50
25
0
-14 -12 -10 -8 -6 -4 -2
hAHR
hAHR-V381A
mAHRb
mAHR-A375V
Log (Competitor)
B
Indirubin
% Specific Binding
h-mAHR
m-hAHR
Log (Competitor)
C
WB:
Control
hAHR
hAHR-V381A
mAHRb
mAHR-A375V
h-mAHR
m-hAHR
α-AHR
α-β -Actin

Fig. 6

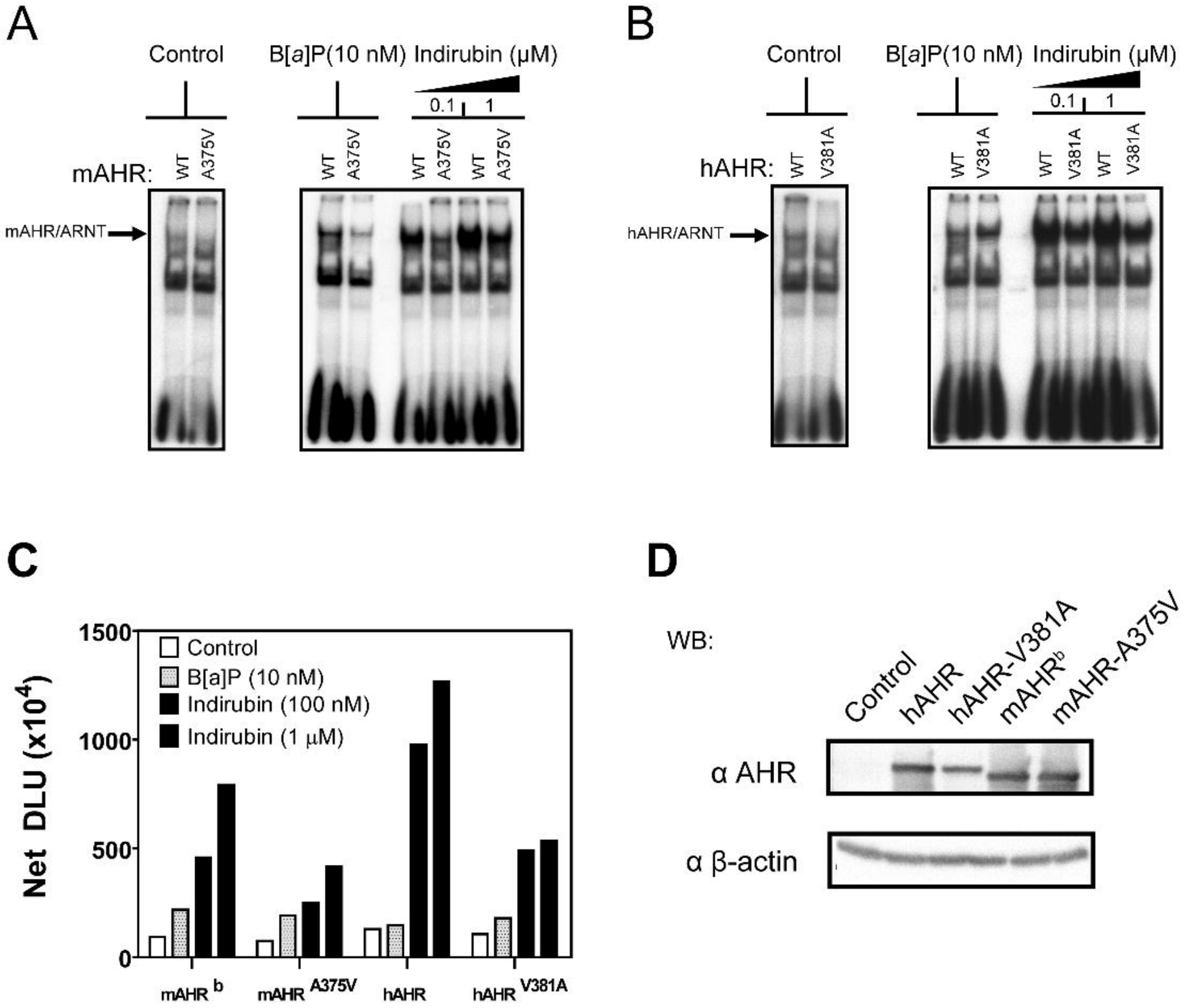
A
Control
B[a]P(10 nM)
Indirubin (μM)
0.1
1
mAHR:
WT
A375V
mAHR/ARNT
B
Control
B[a]P(10 nM)
Indirubin (μM)
0.1
1
hAHR:
WT
V381A
hAHR/ARNT
C
Net DLU (x10^4)
1500
1000
500
0
Control
B[a]P (10 nM)
Indirubin (100 nM)
Indirubin (1 μM)
mAHR b
mAHR A375V
hAHR
hAHR V381A
D
WB:
Control
hAHR
hAHR-V381A
mAHRb
mAHR-A375V
α AHR
α β-actin